

## **A Simultaneous Solution of the Gilbert Equation and its equivalent Landau-Lifshitz-Gilbert Equation**

\*Messaoud Boufligha, \*\*Sebti Boukhtache

\* Department of Electrical Engineering, Faculty of Technology, University of Batna  
Rue Chahid Med El-Hadi Boukhlouf, 05000, Batna, Algeria (messaoud.boufligha@yahoo.fr)

\*\* Department of Electrical engineering, Faculty of technology, University of Batna  
Rue Chahid Med El-Hadi Boukhlouf, 05000, Batna, Algeria (sebti\_boukhtache@yahoo.fr)

### **Abstract**

We present an attempt of a development of at home FORTRAN and Matlab micromagnetic codes based respectively on solving the Gilbert and the Landau-Lifshitz-Gilbert (LLG) equations. These equations are respectively time-integrated by the Cash-Karp-Runge-Kutta (CKRK) algorithm with a customized number of trials (NT) in adapting step size and the standard Runge-Kutta (RK) method. In space, the finite difference method is employed. The previous tools are used in the simulations of the magnetization reversal in a Permalloy thin film, with thermal effects. These simulations have confirmed that the magnetization reversal is depended on the cell size. The (NT) has an impact on the computational time at reduced size. The results given by the solvers showed a slight discrepancy. The validation of our programs is limited to ensuring the correctness of the implementation of the above equations and the employed time-integration methods. For this purpose, the Larmor-precession frequency test is used.

### **Key words**

Thin film; micromagnetic codes; magnetization reversal; thermal effects.

### **1. Introduction**

Ferromagnetic thin films have become important because of their presence in sensors, read/write heads and storage devices. Furthermore, micromagnetic calculation has evolved for optimizing properties of magnetic structures on the nano and micro scales. It is well known that by combining the classical micromagnetic theory with dynamic descriptions of magnetization, one can

simulate the complete magnetization process. This leads to the solution of the Gilbert or its equivalent (LLG) equations which allow us to get information at time-spatial scales that are not accessible experimentally. Unfortunately, these equations have a non linear character. They can only be treated with numerical methods. It is interesting to note that several groups have developed their own versions of codes, based on solving the above equations. Some of them are free, such as Magpar [1], Nmag [2], OOMMF [3], some are commercial, such as LLGsimulator[4], Micromagus [5]. Much effort has been focused on how to include thermal effects in the analysis of the magnetization process. Pioneering investigations were carried out by Neel [6] who studied the influence of thermal fluctuations on the magnetization of fine ferromagnetic particles. Using the Langevin dynamics, Brown [7] gave a first insight into magnetization reversal of a single-domain particle by thermal fluctuations. He came up with the idea of adding a stochastic field to the effective field in the micromagnetic equations. The use of the previous simulation packages is influenced by many requirements as well as the necessary user license, scripting support, the chosen discretization method, the programming language and interface libraries. Recently, researchers have shown increasing interest in the coupling between magnetism and other effects such as conduction, thermal and magnetoelastic effects. Thus, the flexibility of simulation tools becomes a necessity. In this paper, we present an attempt of a development of customized FORTRAN and Matlab codes. The development is based on solving the Gilbert and its equivalent (LLG) equations. They are respectively time-integrated using the Cash-Karp-Runge-Kutta (CKRK) algorithm with a customized number of trials (NT) in adapting time step size control and the standard (RK) method [8,9]. In space, they are discretized by the finite difference method which helps in implementing the Fast Fourier Transform (FFT) technique for demagnetizing field calculations [10]. The analysis of the magnetization reversal at finite temperature in a Permalloy thin film,  $\text{Ni}_{80}\text{Fe}_{20}$  using our own developed tools is achieved. To validate our solvers, we are interested in this paper only to check the correctness of the implementation of the two equivalent equations and the employed time-integration methods by the use of the Larmor-precession frequency test. The present paper is organized as follows: after the introduction in section 1, some details about the used micromagnetic model and the simulation algorithm are presented in section 2. The simulation results, discussion, the partial validation are summarized in section 3. The paper is closed with conclusions.

## 2. Model and simulation details

Theoretical micromagnetics as founded by W. F. Brown allows us to evaluate the total magnetic free energy,  $E_{\text{tot}}$ , of any ferromagnetic body if geometry, material parameters are known. It is the sum of four energy terms

$$E_{tot} = E_{exch} + E_{anis} + E_{dem} + E_{ext} \quad (1)$$

Where

- $E_{exch}$  is exchange energy: It is related to the formation of the domain wall,
- $E_{anis}$  is magnetocrystalline energy: It is closely associated with the crystallographic directions along which the magnetic moments are aligned,
- $E_{dem}$  is magnetostatic energy: It originates from the long-range dipole-dipole interactions, and
- $E_{ext}$  is the energy due to an external field: It forces the magnetization to become oriented in field directions.

The analysis of the magnetization process in ferromagnetic thin films begins with the solution of the micromagnetic equations. For static problems [11] the solution is given by

$$M \times H_{eff} = 0 \quad (2)$$

Whereas, for dynamic problems, the solution is given by the Gilbert equation

$$\frac{dM}{dt} = -\gamma(M \times H_{eff}) + \frac{\alpha}{M_s} \left( M \times \frac{dM}{dt} \right) \quad (3)$$

Or its equivalent (LLG) equation

$$\frac{dM}{dt} = -\frac{\gamma}{1+\alpha^2} (M \times H_{eff}) - \frac{\alpha\gamma}{(1+\alpha^2)M_s} M \times (M \times H_{eff}) \quad (4)$$

Where

- $M$  is the magnetic moment per unit volume,
- $\gamma$  corresponds to the gyromagnetic ratio,
- $\alpha$  denotes the damping parameter,
- $M_s$  is the magnitude of the magnetization, and
- $H_{eff}$  is the effective field: It is the variation of the total free energy with respect to the magnetization and is given by

$$H_{eff} = -\frac{1}{\mu_0} \frac{\delta E_{tot}}{\delta M} \quad (5)$$

$\mu_0$  being the magnetic permeability of the vacuum.

When analyzing a time-dependent magnetization process at finite temperature, a stochastic thermal field  $H_{\text{therm}}$  is added to the effective field. It is defined by

$$H_{\text{therm}} = G \sqrt{\frac{2k_b T \alpha}{\mu_0 \gamma V M_s \Delta t}} \quad (6)$$

Where

- $\Delta t$  is the simulation time-step,
- $K_b$  is the Boltzmann constant,
- $T$  is the temperature of the sample,
- $V$  is the volume of the computational cell, and
- $G$  is a random three-dimensional vector.

This thermal field accounts for the interactions of the magnetization with the microscopic degrees of freedom which cause fluctuations of the magnetization distribution. The thermal field satisfies the following statistical properties

$$\langle H_{\text{therm},i}(t) \rangle = 0 \quad (7)$$

$$\langle H_{\text{therm},i}(t), H_{\text{therm},j}(t') \rangle = 2D \delta_{ij} \delta(t - t') \quad (8)$$

Where  $i, j$  are Cartesian indices. The Kronecker  $\delta_{ij}$  expresses the fact that different components of the thermal field are uncorrelated. The Dirac function shows that the autocorrelation time of the thermal field is much shorter than the response time of the system. The constant  $D$  measures the strength of the thermal fluctuations. The equations can be numerically discretized in space by using either finite difference method, where the thin film is divided into regular cells, or the finite element method, where the cell can take any shape. In this work, the former method is used. The thin film is discretized into a regular two-dimensional grid of square cells. The three-dimensional moments are positioned at the centers of these cells. We assume a uniform distribution of magnetic moments. Spherical coordinates are used in solving Eq. (3), whereas Cartesian coordinates are used in solving Eq. (4). In this section we are interested only to the Gilbert equation details. The moment within one cell can be expressed as

$$M = M_s (\sin \theta \cos \varphi, \sin \theta \sin \varphi, \cos \theta) \quad (9)$$

Where  $\theta$  and  $\varphi$  are respectively the polar and azimuthally angles. When the moment  $M$  rotates by a small amount ( $\Delta\theta$ ,  $\Delta\varphi$ ) [12], a variation in the total free energy occurs. Consequently, the polar and azimuthally components of the effective field are

$$H_{\theta} = -\frac{1}{M_s} \frac{\delta E_{tot}}{\delta \theta} \quad (10)$$

$$H_{\varphi} = -\frac{1}{M_s \sin \theta} \frac{\delta E_{tot}}{\delta \varphi} \quad (11)$$

Carrying out the vector products in Eq. (3) leads to the two equations

$$\frac{d\theta}{d\tau} = \alpha H_{\theta} + H_{\varphi} \quad (12)$$

$$\frac{d\varphi}{d\tau} = \frac{1}{\sin \theta} (-H_{\theta} + \alpha H_{\varphi}) \quad (13)$$

Here  $d\tau$  is the dimensionless time step. The reference material used in the simulations is a permalloy thin film  $\text{Ni}_{80}\text{Fe}_{20}$  of size  $L_x \times L_y \times L_z$ , where  $L_x$ ,  $L_y$  and  $L_z$  are respectively the length, the width, and the thickness. The thin film is discretized into  $N_x$ ,  $N_y$  and  $N_z$ , which respectively represent the number of cells along the x, y and z axes. A single cell is considered along the z axis. The cell discretization must be less than the exchange length. The initial magnetization  $M_{initial}$  is chosen oriented along the easy x-axis. An external field is applied in the thin film plane, in the opposite direction of the x-axis. The micromagnetic calculations start with the evaluation of the effective field components,  $H_{\theta}$  and  $H_{\varphi}$ . The computations of the external field, anisotropic and the exchange contributions are easily done. The last contribution is computed by the four nearest-neighbor moments. However, the main difficulty lies in computing the demagnetizing field contribution, and as a result, several advanced methods are used. It is well known that from a magnetostatic point of view, a ferromagnetic body is equivalent either to a distribution of fictive volume and surface magnetic charges or a distribution of magnetic dipoles. The demagnetizing field calculation is based on a three-dimensional dipolar approximation [13]. By using this approximation, the demagnetizing field results in a convolution product between the magnetization  $M$  and the demagnetizing tensor  $TR$

$$H_{dem} = TR * M \quad (14)$$

Here (\*) represents the convolution product. Thus, the demagnetizing field can be computed by a direct product using the direct and inverse Fourier transforms as follows

$$H_{dem} = TF^{-1} ( TF ( TR ).TF ( M )) \quad (15)$$

The direct and inverse Fourier transforms are evaluated by using two subroutines inspired by the A. Garcia algorithm. The sequence generation of the thermal field contribution is at least the second most computationally intensive part in micromagnetic simulations. The Cartesian components, of the three-dimensional vector  $G$ , are uniformly distributed and randomly generated numbers with an updated seed and are converted into a Gaussian distribution using the Box-Muller transform. They are then transformed to spherical coordinates. The result is added to the previous contributions of the components  $H_\theta$  and  $H_\phi$ . Knowing these components; we start with integrating Eq. (12) and Eq. (13) with respect to time by using the (CKRK) algorithm. The time evolution of the magnetization is obtained by computing the variation in the magnetization angles  $\theta$  and  $\phi$ . For each time step, the effective field is recalculated since it varies with the magnetic distribution. A step is accepted if this variation is below a desired accuracy  $\epsilon$ , with a customized (NT). The micromagnetic model is implemented using the following algorithm, (for more details, see appendix).

Step 1 - set up initial conditions and material parameters.

Step 2 - computation of contributions of effective field.

Step 3 - temporal integration of the corresponding equation and normalization of magnetization vectors.

Step 4 - stopping criterion.

If step 4 is satisfied, go to step 5, else repeat from step 2 to step 4.

Step 5 - computation of average magnetization and stop.

### 3. Results and discussion

As stated earlier, the initial state was chosen with the magnetization oriented along the x-axis. All of our simulations were performed on the reference material. The later, is a thin film,  $Ni_{80}Fe_{20}$  measuring  $160 \times 80 \times 5 \text{ nm}^3$ . The intrinsic material parameters used are those found in the literature, i.e., the exchange constant  $A = 1.3 \times 10^{-11} \text{ J/m}$ , the saturation magnetization  $M_s = 8.0 \times 10^5 \text{ A/m}$  and the uniaxial anisotropy constant,  $K_u = 0 \text{ J/m}^3$  while the dynamic parameters  $\gamma$  and  $\alpha$  have been set equal to  $2.21 \times 10^5 \text{ m/ (As)}$  and 0.08, respectively. The simulations has been carried out using  $2.5 \times 2.5 \times 2.5 \text{ nm}^3$  and  $5 \times 5 \times 5 \text{ nm}^3$  cells. An external field of 150 kA/m is applied in the thin film plane, in the opposite direction of the x-axis. The reversal state is defined as the average magnetization when it attained 90% in the direction of the external field. The desired accuracy,  $\epsilon$ , is set to  $10^{-9}$

Let us now focus on the solution of Eq. (3) in the case of zero temperature. Fig. 1 shows the time evolution of the average magnetization  $\langle M_x \rangle$ .

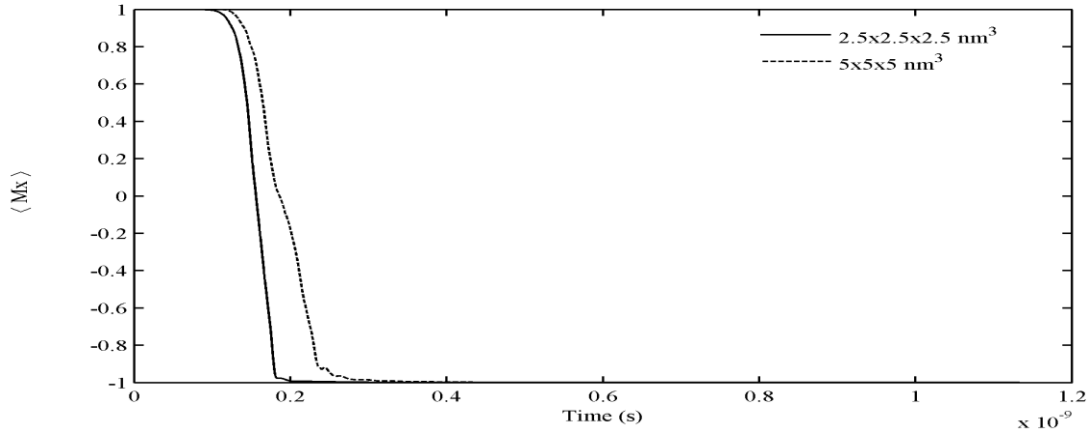


Fig. 1 Time evolution of the average magnetization  $\langle M_x \rangle$  during the reversal process in the thin film discretized in cells of sizes  $2.5 \times 2.5 \times 2.5 \text{ nm}^3$  and  $5 \times 5 \times 5 \text{ nm}^3$ .

It is worth noting that after applying the external field, the average magnetization,  $\langle M_x \rangle$ , remained constant and reached the reversal state for shorter periods of time for the thin film with the small cell size as compared to the case with the large cell size. As a result, the speed of the magnetization reversal process is increased when the cell size was reduced. The used integrating scheme is characterized by an automatic selection and an updating of the time step. Therefore, it leads during the computation of the reversal magnetization to a set of failed and successful steps to satisfy the desired accuracy. Fig. 2 and Fig. 3 show respectively the time evolution of the number of failed steps, (NFSteps) and the number of successful steps, (NSSteps) for different (NT).

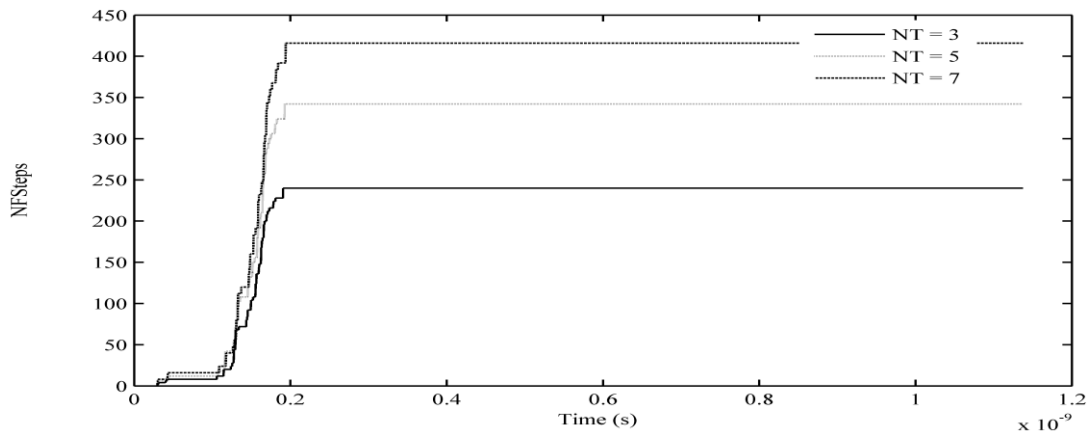


Fig. 2 Time evolution of the NFSteps during the computation of the reversal magnetization in the thin film discretized in cells of size  $5 \times 5 \times 5 \text{ nm}^3$  for different (NT).

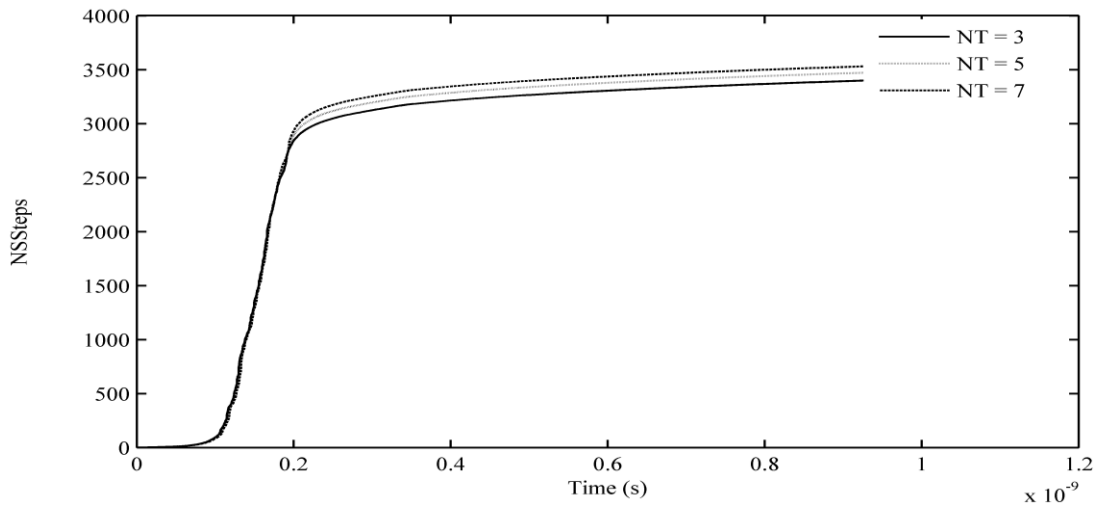


Fig.3 Time evolution of the NSSSteps during the computation of the reversal magnetization in the thin film discretized in cells of size  $5 \times 5 \times 5 \text{ nm}^3$  for different (NT).

It is observed that the increase of the (NT) causes an increase of the number of failed and successful steps. The use of smaller cell size has an impact on the calculation time. According to Fig. 4 and Fig. 5 where the cell size used is of  $2.5 \times 2.5 \times 2.5 \text{ nm}^3$ , and despite the decrease in the desired accuracy which is set to  $10^{-7}$ , the numbers of failed and successful steps are drastically increased. Consequently, the computational time is affected.

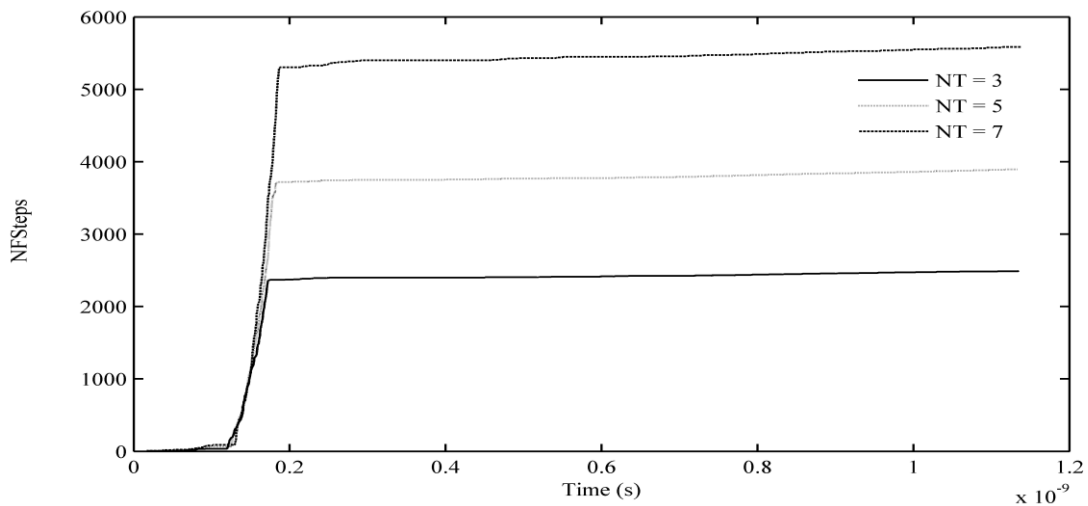


Fig. 4 Time evolution of the NFSSteps during the computation of the reversal magnetization in the thin film discretized in cells of size  $2.5 \times 2.5 \times 2.5 \text{ nm}^3$  for different (NT).

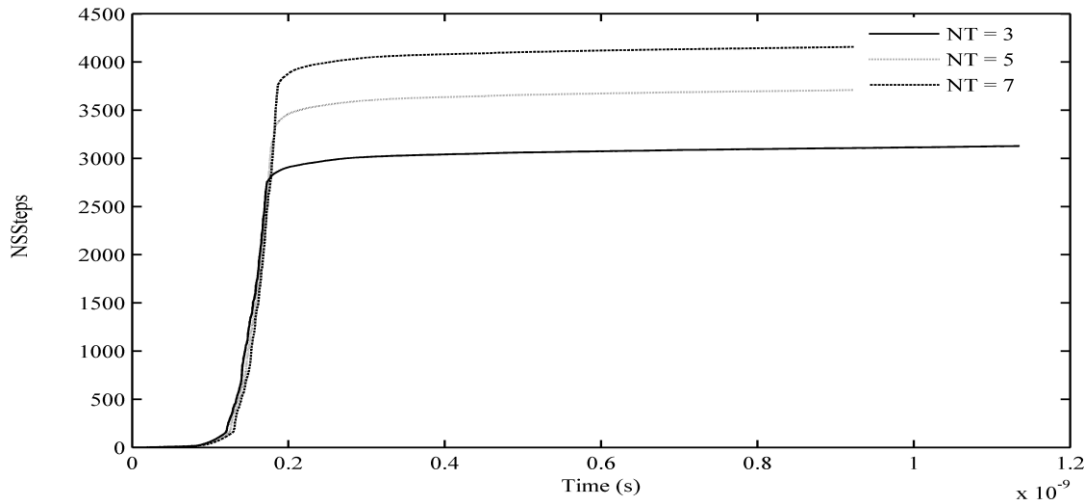


Fig. 5 Time evolution of the NSSSteps during the computation of the reversal magnetization in the thin film discretized in cells of size  $2.5 \times 2.5 \times 2.5 \text{ nm}^3$  for different (NT).

So far, we have only discussed the influence of the discretization cell size on the magnetization process and the impact of the (NT) on the computational time. In this part, we show the dependence of the speed of the magnetization process on the size-thermal effects. For this purpose, a thermal field is added to the effective field. The simulations were carried out on the thin film, at both  $T = 0 \text{ K}$  and  $T = 350 \text{ K}$ , using separately the two different discretizations. Fig. 6 shows the time evolution of the average magnetization  $\langle M_x \rangle$ .

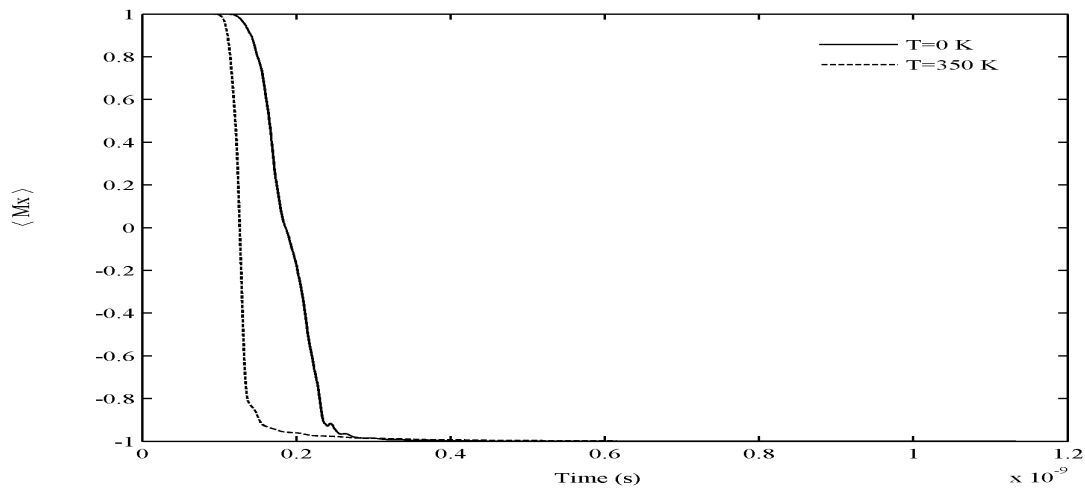


Fig. 6 Time evolution of the average magnetization  $\langle M_x \rangle$  during the reversal process in the thin film discretized in cells of size  $5 \times 5 \times 5 \text{ nm}^3$  at  $T = 0 \text{ K}$  and  $T = 350 \text{ K}$

Similarly, as in the case where thermal effects were neglected, it is important to note that after applying the external field, including thermal effects tends to shorten the reversal time

As a result, the speed of the magnetization reversal process also increases when the temperature is increased. Thermal fluctuations allow magnetization to rotate out of its preferred orientation [14]. When the discretization cell size decreases, i.e. in the case of  $2.5 \times 2.5 \times 2.5 \text{ nm}^3$  cells, the thermal effects can be clearly seen as shown in Fig. 7. That is why several works have addressed the dependence of numerical results on the cell size [15, 16].

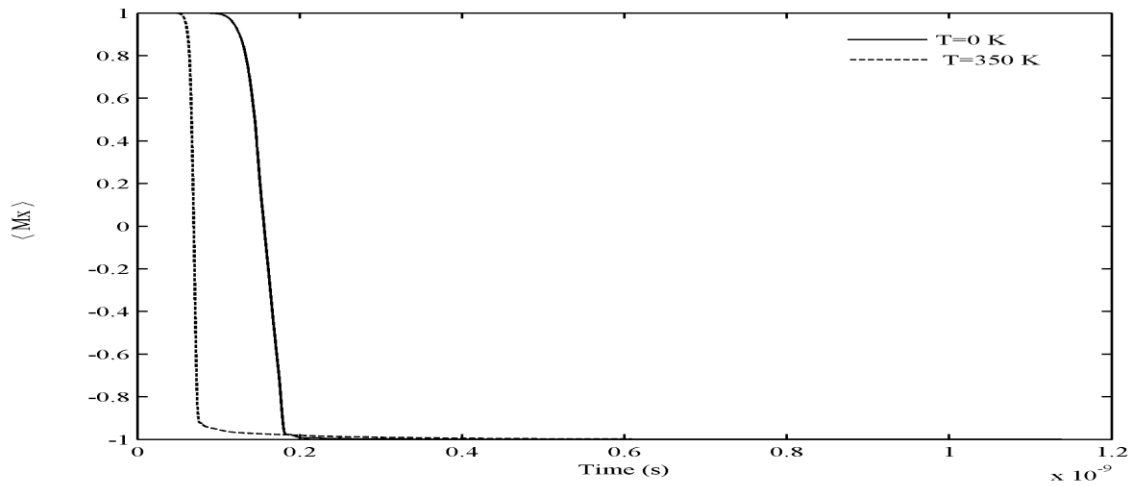


Fig. 7 Time evolution of the average magnetization  $\langle M_x \rangle$  during the reversal process in the thin film discretized in cells of size  $2.5 \times 2.5 \times 2.5 \text{ nm}^3$  at  $T = 0 \text{ K}$  and  $T = 350 \text{ K}$ .

All the above simulations were performed by the use of the FORTRAN code. Let us now choose an intermediate  $NT = 5$  and a desired accuracy,  $\epsilon = 10^{-9}$ . Fig. 8 summarizes a comparison between the previous simulations at  $T = 0 \text{ K}$  and those given by the solution of Eq. (4) performed by the Matlab code.

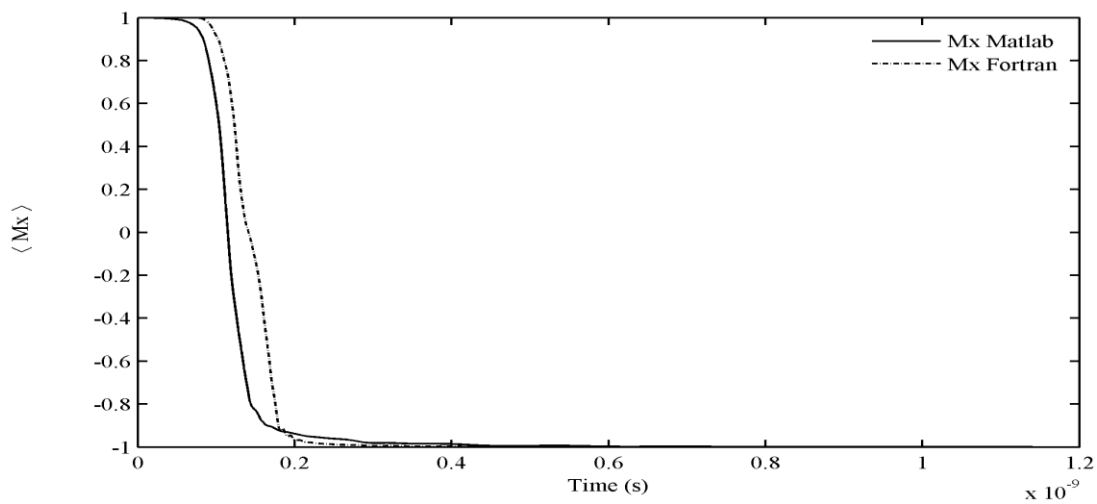


Fig. 8 Time evolution of the average magnetization  $\langle M_x \rangle$  during the reversal process in the thin film discretized in cells of size  $5 \times 5 \times 5 \text{ nm}^3$ , computed by our codes at  $T=0 \text{ K}$

It can be observed that the reversal state is reached quietly at the same time. The slight discrepancy between the trajectories obtained by the simulations performed by the two versions of programs is attributed to the following reasons: the used time-integration schemes are different as state earlier. The FFT methods are different; i.e., in the first tool, the direct and inverse Fourier transforms are evaluated by using two subroutines inspired by the A. Garcia algorithm while we employed the Matlab functions `fft2d` and `ifft2d` in the second program. Furthermore, the two equations solved are equivalent but are not the same.

To ensure the correctness of the implementation of Eq. (3), Eq. (4) and the employed time-integration methods, the Larmor-precession test frequency is used. The test starts from a magnetization uniformly in the direction (1,1,1). The damping parameter is set to zero, while the gyromagnetic ratio is kept equal to  $2.21 \times 10^5$  m/(As). The only contribution to the effective magnetic field is the external field. It takes a value of  $10^6$  A/m in the z-direction. Fig. 9 presents the results of the test simulated by our own codes.

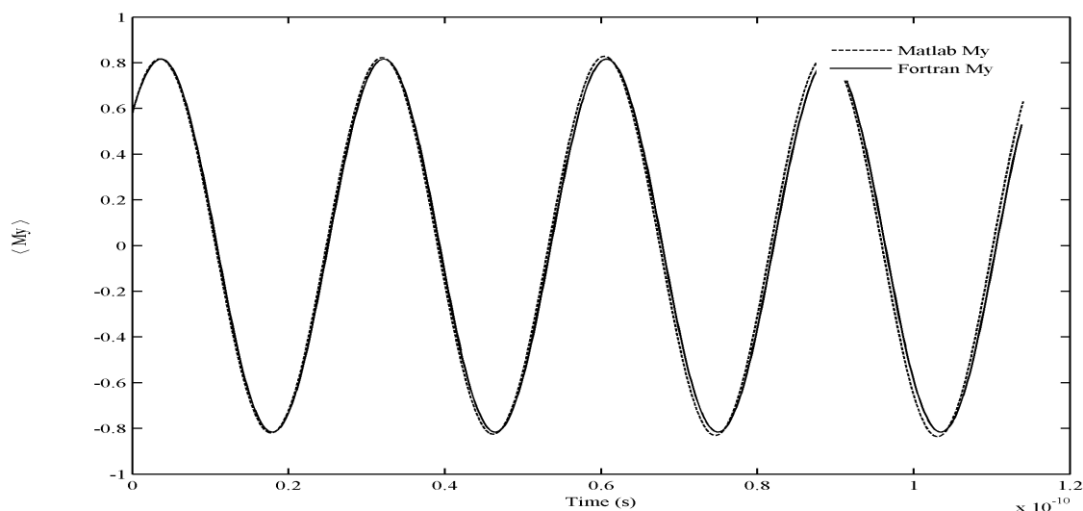


Fig. 9 Time evolution of the average magnetization  $\langle My \rangle$  given by the Larmor-precession test and computed using FORTRAN and Matlab codes.

The frequency of the precession which is depended on the strength of the effective field [17] is determined by a fit of the average magnetization component  $\langle My \rangle$  over time using a sine function. It can be observed that the period of this function matches the Larmor precession of  $T=28.42847$  ps. The results are in agreement with those presented in the literature.

## Conclusions

Two customized FORTRAN and Matlab codes have been developed based on solving both the Gilbert and its equivalent equations. The magnetization reversal at zero and a finite temperature in a permalloy thin film is analyzed using these tools. It is worth to note that the magnetization reversal process is dependent on the cell size. The (NT) has an impact on the computational time at reduced sizes. The slight discrepancy between the results obtained by the Matlab and the FORTRAN programs is justified. A limited validation is carried out. Strong agreement is achieved between our results and those presented in the literature. We would like to mention that a flexibility to extend these tools and including others effects is allowed.

## Acknowledgment

The authors warmly thank Mr. A. Bouchtob, lecturer at the University of Batna for his help and assistance.

## References

1. [www.magnet.atp.tuwien.ac.at.sholtz/magpar](http://www.magnet.atp.tuwien.ac.at.sholtz/magpar),access date April 2010.
2. [www.nmag.soton.ac.uk](http://www.nmag.soton.ac.uk),access date January 2012.
3. [www.math.nist.gov/oommf/](http://www.math.nist.gov/oommf/),access date April 2014.
4. [www.llgmicro.home.mindspring.com/](http://www.llgmicro.home.mindspring.com/), access date April 2015.
5. [www.micromagus.de/](http://www.micromagus.de/),access date January 2016.
6. L.Neel,"Influence des fluctuations thermiques sur l'aimantation des grains ferromagnétiques très fins", Comptes rendus,vol. 228, pp. 664-666, 1949.
7. W. F. Brown," Thermal fluctuations of a single-domain particle", Phys. Review, vol.130, issue 5, pp. 1677-1686, 1963.
8. A. Romeo, G. Finocchio, M. Carpentieri, L.Torres, G. Consolo, B. Azzerboni, "A numerical solution of the magnetization reversal modeling in a permalloy thin film using a fifth order Runge-Kutta method with adaptive step- size control", Physica B. 403, pp. 464-468, 2008.
9. Novikov, E.A,"Runge kutta explicit methods: Algorithm of variable order and steps", [www.amse-modeling.org](http://www.amse-modeling.org), access date February 2016.
10. [www.garcia.org/nummeth/nummeth](http://www.garcia.org/nummeth/nummeth) , access date June 2014.
11. H. Kronmüller, R. Hertal, "Computational of magnetic structures and magnetization processes in small particles", J.Magn.Magn.Mat.vol.215-216, pp. 11-17, 2000.
12. M. Mansuripur, "The physical principles of magneto- optical Recording", Cambridge university press, 1995.

13. Y. Nakatani, Y. Uesaka, N. Hayachi, "Direct solution of the Landau-Lifshitz-Gilbert equation for micromagnetics", Japanese Journal of Applied Physics.vol 28,No.12 ,pp. 2485-2507, 1989.
14. V. Tsiantos, W. Scholz, D. suess, T. Schrefl , J. Fidler," The effect of the cell size in langevin micromagnetic simulations ", J.Magn.Magn.Mat.vol.242-245, pp. 999-1001, 2002.
15. E. Matinez,L.Lopez-Diaz,L.Torres,C.J.Garcia-Cervera,"Minimizing cell size dependence in Micromagnetics with thermal noise",J. Physics D:Appl. phys vol.40,No.4,pp.942-948,2007
16. J. Fidler,T. Shrefl,V.Tsiantos,W. Scholz,D.Suess, "Micromagnetic simulation of the magnetic switching behavior of mesoscopic and nanoscopic structures",computational materials science,vol.24,pp.163-174,2002
17. J. Stohr, H.C. Siegmann,"Magnetism from fundamentals to nanoscale dynamics",Springer-Verlag, Berlin Heidelberg, 2006.

## Appendix

It is worth to mention that in this paper we are dealing with a 2D problem, i.e., one cell in the  $z$ -direction as represented by fig.1A.

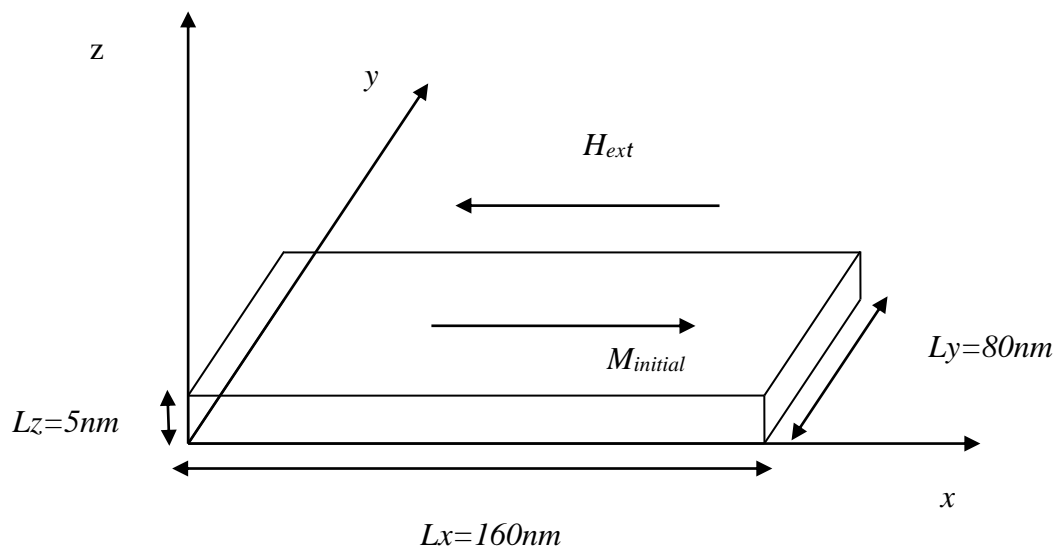


Fig. 1A. The geometry of the thin film

The magnetization in a computational cell,  $(\Delta x, \Delta y, \Delta z)$  is indexed by  $(i, j)$  in 2D and represented in Cartesian coordinates by

$$M = (M_x, M_y, M_z) \quad (1.A)$$

And in spherical coordinates by Eq.(9). The cell size is defined by

$$\begin{aligned} \Delta x &= L_x / N_x \\ \Delta y &= L_y / N_y \\ \Delta z &= L_z / N_z \end{aligned} \quad (2.A)$$

The change of the magnetization is caused by the total effective magnetic field

$$H_{eff} = H_{exch} + H_{anis} + H_{dem} + H_{ext} \quad (3.A)$$

Where  $H_{exch}$ ,  $H_{anis}$ ,  $H_{dem}$  and  $H_{ext}$  are the standard contributions to the total effective field at zero temperature. However, at a finite temperature the thermal field,  $H_{therm}$  is added.

The demagnetizing field contribution is firstly obtained by calculation of the demagnetizing tensor defined by the matrix, TR composed by nine demagnetizing coefficients.

$$TR = \begin{pmatrix} TR_{xx} & TR_{xy} & TR_{xz} \\ TR_{yx} & TR_{yy} & TR_{yz} \\ TR_{zx} & TR_{zy} & TR_{zz} \end{pmatrix} \quad (4.A)$$

These coefficients are evaluated using these formulas in the three dimensional case

$$TR_{xx}(I, J, K) = \sum_{\alpha=0}^1 \sum_{\beta=0}^1 \sum_{\gamma=0}^1 (-1)^{\alpha+\beta+\gamma} \tan g^{-1} \left| \frac{(K + \gamma - 0.5)(J + \beta - 0.5)\Delta z \Delta y}{r(I + \alpha - 0.5)\Delta x} \right| \quad (5.A)$$

$$TR_{xy}(I, J, K) = TR_{yx} = - \sum_{\alpha=0}^1 \sum_{\beta=0}^1 \sum_{\gamma=0}^1 (-1)^{\alpha+\beta+\gamma} \log |(K + \gamma - 0.5)\Delta z + r| \quad (6.A)$$

Where

$$r = \sqrt{(I + \alpha - 0.5)^2 \Delta x^2 + (J + \beta - 0.5)^2 \Delta y^2 + (K + \gamma - 0.5)^2 \Delta z^2} \quad (7.A)$$

The other coefficients can be obtained by the simultaneous cyclic permutations of  $(I, J, K)$ ,  $(\alpha, \beta, \gamma)$  and  $(\Delta x, \Delta y, \Delta z)$ .

The computation of the demagnetizing tensor, TR is done using Cartesian coordinates in the case of the use both the two codes.

▪ **In Matlab code**

The Cartesian coordinates are used to express all the contributions of the effective field.

- The contribution of the exchange field in a general three dimensional case is represented in Cartesian coordinates by

$$\begin{aligned} H_{exch,x} = & \frac{2A}{M_s^2} \left( \frac{M_x(i+1, j, k) - 2M_x(i, j, k) + M_x(i-1, j, k)}{\Delta x^2} \right) \\ & + \frac{2A}{M_s^2} \left( \frac{M_y(i, j+1, k) - 2M_y(i, j, k) + M_y(i, j-1, k)}{\Delta y^2} \right) \\ & + \frac{2A}{M_s^2} \left( \frac{M_z(i, j, k+1) - 2M_z(i, j, k) + M_z(i, j, k-1)}{\Delta z^2} \right) \end{aligned} \quad (8.A)$$

The other components of the exchange field are obtained by replacing x with y or z in the above equation.

It is worth noting that the evaluation of the exchange field is enforced by the values of the boundary conditions given by

$$\frac{\delta M_x}{\delta n} = \frac{\delta M_y}{\delta n} = \frac{\delta M_z}{\delta n} = 0 \quad (9.A)$$

Where n is the normal to the respective direction.

- The contribution of the anisotropy field is defined by

$$H_{anis} = -\frac{2K_u}{\mu_0 M_s^2} M \quad (10.A)$$

- The contribution of the external is uniform in each computational cell
- The contribution of the demagnetizing field is computed using Eq. (15), where the functions `fft2d` and `ifft2d` in Matlab are used respectively to compute (TF) and (TF<sup>-1</sup>).

Considering the reduced, form. Therefore,  $h = \frac{H}{M_s}$ ,  $m = \frac{M}{M_s}$  and  $d\tau = dt\gamma M_s$ , So

- $h_x, h_y$  and  $h_z$  are the reduced components of the total effective field ,
- $m_x, m_y$  and  $m_z$  are the reduced components of the magnetization.

The time integration of the three equations below is achieved using the standard Runge Kutta method according to the simple algorithm presented in section.2.

$$\frac{dm_x}{d\tau} = -\frac{1}{1+\alpha^2} \left[ (m_y h_z - m_z h_y) + \alpha m_y (m_x h_y - m_y h_x) - \alpha m_z (m_z h_x - m_x h_z) \right] \quad (11.A)$$

$$\frac{dm_y}{d\tau} = -\frac{1}{1+\alpha^2} \left[ (m_z h_x - m_x h_z) + \alpha m_z (m_y h_z - m_z h_y) - \alpha m_x (m_x h_y - m_y h_x) \right] \quad (12.A)$$

$$\frac{dm_z}{d\tau} = -\frac{1}{1+\alpha^2} \left[ (m_x h_y - m_y h_x) + \alpha m_x (m_z h_z - m_x h_x) - \alpha m_y (m_y h_z - m_z h_y) \right] \quad (13.A)$$

#### ▪ In Fortran code

The spherical coordinates are used to express all the contributions of the effective field using Eq.(10) and Eq.(11).

- the components of the contribution of the anisotropic field

If the local axe of the anisotropy has an arbitrary direction,  $u_0$  specified by the angles  $(\theta_0, \varphi_0)$  and a moment,  $M$  has a direction,  $u_r$  specified by the angles  $(\theta, \varphi)$ . Furthermore, the anisotropy energy density is expressed as

$$e_{anis} = K_u \left[ 1 - (u_r \cdot u_0)^2 \right] \quad (14.A)$$

So, the components are expressed as

$$H_{\theta_{anis}} = -\frac{K_u}{M_s} \left\{ \sin 2\theta [\cos^2 \theta_0 - \sin^2 \theta_0 \cos^2(\varphi - \varphi_0)] - \cos 2\theta \sin 2\theta_0 \cos(\varphi - \varphi_0) \right\} \quad (15.A)$$

$$H_{\varphi_{anis}} = -\frac{K_u}{M_s} \left[ \sin \theta \sin^2 \theta_0 \sin 2(\varphi - \varphi_0) + \cos \theta \sin 2\theta_0 \sin(\varphi - \varphi_0) \right] \quad (16.A)$$

- the spherical components of the exchange field contribution

If we considered two nearest neighbors moments,  $M$  and  $M_1$  speared by a distance,  $d$ , the exchange energy density is expressed as

$$e_{exch} = \frac{2A}{d^2} \left( 1 - \frac{M}{|M_s|} \cdot \frac{M_1}{|M_s|} \right) \quad (17.A)$$

So, the components are expressed as

$$H_{\theta_{exch}} = -\frac{2A}{M_s d^2} [\sin \theta \cos \theta_1 - \cos \theta \sin \theta_1 \cos(\varphi - \varphi_1)] \quad (18.A)$$

$$H_{\varphi_{exch}} = -\frac{2A}{M_s d^2} \sin \theta_1 \sin(\varphi - \varphi_1) \quad (19.A)$$

- The spherical components of the external field contribution are easily obtained by a simple spherical conversion of their Cartesian components

$$H_{\theta_{ext}} = H_x \cos \theta \cos \varphi + H_y \cos \theta \sin \varphi - H_z \sin \theta \quad (20.A)$$

$$H_{\varphi_{ext}} = -H_x \sin \varphi + H_y \cos \varphi \quad (21.A)$$

- The components of de demagnetizing field are determined firstly in Cartesian coordinates using Eq. (15). For this purpose, the inspired subroutines, `fft2d` and `ifft2d` are adapted by the implementation of the zero-padding algorithm. In the one-dimensional case,(x-direction, for example), the number of elements stoked in both, the demagnetizing coefficients and the components of  $M$  are extended to  $2N_x$  instead of  $N_x$  which is the number of cells in x-direction. The additional elements are replaced by zero. The zero-padding algorithm is done in three steps:
  - Calculate both the discrete Fourier transforms of the all the demagnetizing coefficients and the components of  $M$
  - Calculate the product of these discrete Fourier transforms, element by element.

- Calculate the inverse discrete Fourier transform of this product. Only, the elements of the results indexed from 0 to N-1 are retained. These elements represent,  $H_{demx}$ , ( $H_{demy}$  and  $H_{demz}$ ). The results are converted to spherical coordinates, in order to obtain  $H_{dem\theta}$  and  $H_{dem\varphi}$ . When the spherical components of the total effective field are determined, we proceed to the time integration of Eq.(12) and Eq.(13) using the cash Karp Runge Kutta algorithm with a customized number of trials in step size control according to the simple algorithm mentioned in section.2.